ORIGINAL ARTICLE

Neural Network based Control Method Implemented on Ambidextrous Robot Hand

Mashood Mukhtar[1,*], Emre Akyürek[1], Tatiana Kalganova[1] and Nicolas Lesne[2]

[1]*Department of Electronic and Computer Engineering, Brunel University, Kingston Lane, Uxbridge, London, UK*

[2]*Department of System Engineering, ESIEE Paris, Noisy-le-Grand Cedex, France*

(**Received** 11 May 2016; **Accepted** 20 September 2016; **Published on line** 1 March 2017)

*Corresponding author: Mashood.Mukhtar@brunel.ac.uk

DOI: 10.5875/ausmt.v7i1.1171

Abstract: Human hands can precisely perform a wide range of tasks. This paper investigates key performance differences when conventional robotic hand controllers are combined with Neural Networks (NN). Tests are performed on a novel 3D printed multi-finger ambidextrous robot hand. The ambidextrous hand is actuated using pneumatic artificial muscles (PAMs) and can bend its fingers both left and right, offering full ambidextrous functionality. Force sensors are placed on the fingertips. In our control method, the grasping trajectory of each finger combines its data with that of the neighboring fingers to obtain accurate results.

Keywords: robot hand, ambidextrous hand design, grasping algorithms, control methods; pneumatic systems, multifinger control, neural network control

Introduction

Robotic manipulators have become increasingly important in the field of flexible automation. Neural Networks (NNs) can flexibly map nonlinear functions. Networks can be trained and applied both on or off-line. Of the many neural network types, two of the most widely used are multi-layer perception (MLP) and radial basis function (RBF) [1]. Back propagation is most popular method of implementing multi-layer perception (MLP). There are three major learning paradigms: supervised learning, unsupervised learning and reinforcement learning. Each learning paradigm is suitable to solving a specific set of problems. A three-layer NN with full interconnections is shown in Figure 1.

The output of the two-layer NN is as follows:

$$y_i = \sigma\left(\sum_{l=1}^{L} w_{il}\sigma\left(\sum_{j=1}^{n} v_{lj}\, x_j + v_{l0}\right) + w_{i0}\right) \quad (1)$$

where i =1, 2, 3,…… …., m, L is the number of neurons, σ is the activation function, and w is weight.

Neural networks have been widely applied in robot control and motion planning [2] [3]. They have been used to achieve motion control of manipulators [4], to help robots follow predetermined trajectories on city streets [5] and to achieve visual control of robotic arms [6]. A real-time learning neural robot controller was used to solve the inverse kinematics problem [7], and an artificial neural network was used to help a robotic arm system with six degrees of freedom to track and grasp a moving object [8].

Neural Networks can be implemented into robotic structures in several ways and with different controllers to provide improved solutions. For instance in [9], a learning process is designed for the two-links PAM manipulator to have an adaptive and dynamic self-organizing structure using NN and fuzzy logic. An NN was connected to PID loops in [10] to create an intelligent phasing plane switch control (PPSC) to overcome nonlinearities in PAM pressure feedback. NNs have also been integrated into particle swarm optimization to increase system accuracy [11].

The present paper combines neural networks with the PID, Bang-bang and Back-stepping algorithms. These controllers (PID, BSC, Bang-bang and SMC) are discussed in great detail in [12]. Table 5 summarizes the controllers combined with NNs and their respective experimental results. Force sensors are implemented on the fingertips of the ambidextrous robot hand. Use of these sensors with intelligent controllers increased robot hand autonomy as the grasping trajectory of each finger is based not only on its own feedback data, but also on that of the closest fingers.

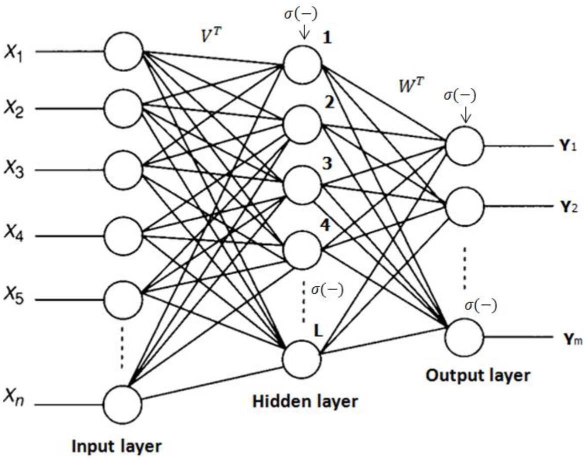

Figure 1. Three layer Neural Network (NN).

Combining Neural Networks with grasping algorithms

Unlike pressure sensors that are connected to PAMs and always detect variations when a robot hand is interacting with objects, force sensors are deployed only on strategic points of the fingers. Therefore, when an object comes into contact with robotic fingers at points not covered by force sensors, the fingers continue to close as directed by the grasping algorithms. A neural network is thus integrated into the grasping algorithm as a security measure. In the following, F_f refers to a force F applied by each of the four other fingers (where f is a notation), F_t is the target force and $F_f(t)$ is the force received from each finger. For the force feedback of each finger $F_f(t)$, the values of the closest fingers $F_{f-1}(t)$ and $F_{f+1}(t)$ are also considered. In case $F_f(t) = 0$ but $F_{f-1}(t)$ or $F_{f+1}(t)$ receives a high force feedback, two different outcomes are possible. Either the object is not in contact with the sensor F_f or the object is not in contact with the finger at all. In the first case, the grasping controller must stop as the finger is actually in contact with the object. In the second case, not all fingers are needed to grasp the object. The detection of this case is translated as follows (where a constant 0.9 is the ratio experimentally defined to react to the object's presence):

$$F_{cf} \geq 0.9 * F_t \quad (2)$$

where $F_{cf} = [F_{f-1}(t) \cup F_{f+1}(t)]$ and $F_f(t) \simeq 0$

If Eq. (2) is true, then at least one of the fingers close to the finger f is close to the object. If Eq. (2) is true and $F_f(t) \simeq 0$, then the object is either not in contact with the sensor or with the finger. So the grasping controller must either stop or make the finger return to its vertical position. In the finger f is in contact with the object, the reacts differently by reading the angular angle. Thus angular feedback is read in reference to the angle of the vertical position. In Eq. 2 F_{cf} refers to adjacent fingers to both sides of concerned finger.

In Eq. 3, $\theta_f(t)$ refers to the angle of each finger and a constant of 0.8 is the ratio experimentally defined to determine whether there is an abnormal increase of grasping angles.

$$\theta_{f-1}(t) < 0.8 * \theta_f(t) \quad (3)$$

and

$$\theta_{f+1}(t) < 0.8 * \theta_f(t) \quad (4)$$

If both (3) and (4) are correct, then the angle of finger f is much smaller than those of its adjacent fingers $f-1$ and $f+1$. Consequently, the more the finger f closes, the bigger $\theta_f(t)$ becomes. Thus, a constant below 1 is used to check if $\theta_{f-1}(t)$ or $\theta_{f+1}(t)$ have stopped increasing at a smaller angle. If the finger f does not touch any objects, then it reverts to its vertical position. $\theta_f(t)$ is then compared to a value close to $\pi/2$ to determine whether finger f is perpendicular to the palm. In so, finger f reverts to its vertical position without contacting any objects. These algorithms are summarized in Fig. 2. F_0 is the thumb, for which the angle is not considered.

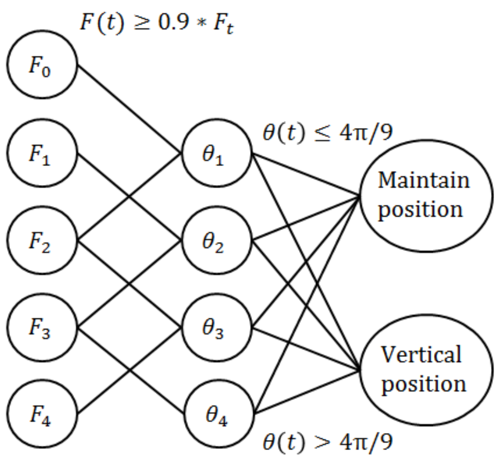

Figure 2. Neural network mapping (from thumb F0 to little finger F4).

Results obtained with NNs

Table 1-4 shows the results obtained with the proposed approach, while Figs. 3 and 4 show the hand grasping a ball and a water bottle. The position of the fingers changes depending on the shape of the object being grasped. Table 1-4 also summarizes the angles and force received by the different fingers during grasping. The force target is 2.25 N ± 10% for the bottle and 1 N ± 5% for the ball. The indicated angles are those of the proximal phalanges.

When the hand grasps the bottle, the fingers come into contact with the object within 0.2 sec, but the angles continue to increase until 0.45 sec because the fingers continue closing until the bottle is pressed up against the thumb on the far side.

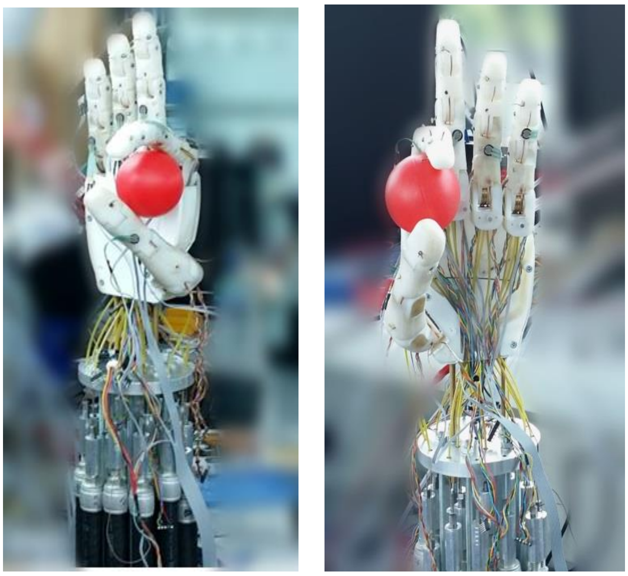

Figure 3. Ambidextrous robot hand holding a ball.

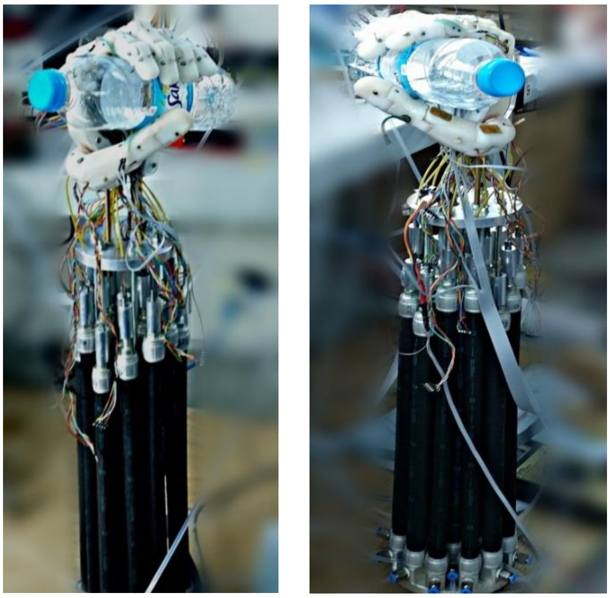

Figure 4. Ambidextrous robot hand holding a water bottle.

The middle finger is longer than the others, thus the force sensor on the tip of the middle finger does not come into contact with the object. However, because of the implemented NN, the force data collected from the neighboring fingers also play key part in the grabbing process as shown by the angle reached in Table 2..

The fingers react in a totally different way when grabbing a ball. The forefinger comes into contact with the object at 0.1 sec and its movement stops at 0.3 sec (as opposed to 0.4 sec for the bottle), as the object is bigger and the target force is smaller. Also, this grabbing action only involves the thumb and forefinger. As seen in Figs. 5 and 6, the different finger shape results in the middle finger having the slowest movement, whereas the little finger is the fastest.

As it applies no force and its angle becomes much smaller than that of the forefinger, it is deduced the middle finger is not in contact with the object. Therefore the finger starts rising before 0.3 sec. Next the NN is applied in the same way to the ring finger at 0.4 sec, and finally the little finger starts returning to its vertical position at 0.5 sec. The little finger moves more slowly than the middle and ring fingers because compressed air is already being used to drive their movement. The speed of the middle and ring fingers barely varies, as the PAM is in the middle of their contraction. Thus, a small increase of pressure still implies an important variation of the PAMs' lengths. The movement speed of the little finger increases at 0.8 sec, when the middle finger approaches the vertical position and has its own speed reduced. The compressed air is therefore only involved in the movements of the ring and little fingers. Finally, only the forefinger maintains its closing position, whereas the middle, ring and little finger return to their vertical positions. While the grabbing movement for the bottle was completed in 0.45 sec, that for the ball took 1 sec because it comprised both closing and opening movements.

Experimental Analysis

Table 5 compares different behaviors observed with other grasping algorithms (SMC, PID, Bang-bang and BSC) developed at earlier stages.

The sliding-mode control (SMC) introduced in [13] uses a grasping loop combined with average rising times, percentages of overshoot, number of oscillations, grasping times and settling times. SMC and other methods differ in significant ways. For instance, SMC runs in parallel, thus the percentage of overshoot is not applicable. The grasping and settling times are the same for the SMC because no backward control is implemented as in bang-bang control. However, the grasping and settling times are different for the bang-bang control because of the algorithm's low sensitivity.Generally, SMC is easier to implement from a mechanical point of view, whereas PID is easier to implement from an algorithmic point of view. The implementation and calibration of grasping algorithms receiving feedback from the force sensors is much faster than from pressure transducers as the hysteresis of PAMs does not need to be taken into account with force sensors.

Table 1. Force (N) against time (sec) at the fingertips when the hand grabs a bottle.

Time	0	0.05	0.1	0.15	0.2	0.25	0.3	0.35	0.4	0.45
Forefinger	88	79	65	39	30	25	18	13	9	9
Middle finger	93	84	75	44	32	27	20	11	10	8
Ring finger	86	76	67	36	29	23	16	11	10	9
Little finger	85	69	57	34	28	20	13	9	8	8

Table 2.Finger angles (deg) against time (sec) when the hand grabs a bottle.

Time	0	0.05	0.1	0.15	0.2	0.25	0.3	0.35	0.4	0.45
Forefinger	88	79	65	39	30	25	18	13	9	9
Middle finger	93	84	75	44	32	27	20	11	10	8
Ring finger	86	76	67	36	29	23	16	11	10	9
Little finger	85	69	57	34	28	20	13	9	8	8

Table 3. Force (N) against time (sec) at the fingertips when the hand grabs a ball.

Time	0	0.05	0.1	0.15	0.2	0.25	0.3	0.4	0.5	0.6	0.7	0.8	0.9	1
Forefinger	0	0	0.3	0.8	0.99	1.05	1.06	1.06	1.04	1.05	1.03	1.04	1.04	1.04
Middle finger	0	0	0	0	0	0	0	0	0	0	0	0	0	0
Ring finger	0	0	0	0	0	0	0	0	0	0	0	0	0	0
Little finger	0	0	0	0	0	0	0	0	0	0	0	0	0	0

Table 4. Finger angles (deg) against time (sec) when the hand grabs a ball.

Time	0	0.05	0.1	0.15	0.2	0.25	0.3	0.4	0.5	0.6	0.7	0.8	0.9	1
Forefinger	93	82	56	38	27	20	20	20	19	19	19	19	19	19
Middle finger	88	83	64	43	25	12	16	31	44	60	73	87	91	87
Ring finger	90	79	49	27	5	0	0	9	23	46	65	82	85	84
Little finger	87	75	47	26	3	3	3	3	7	17	39	72	86	86

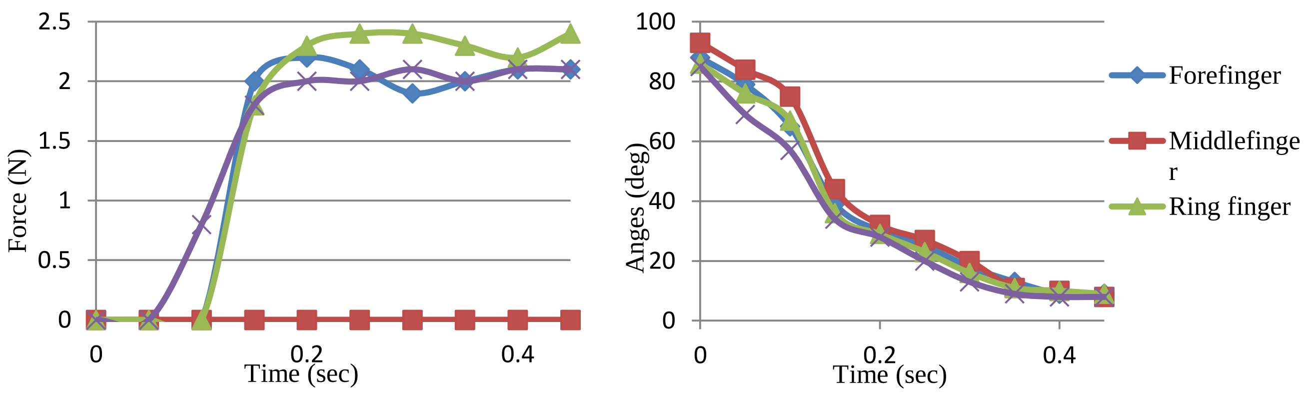

(a) (b)

Figure 5. Finger forces and angles against time when the hand grabs a ball.

Bang-bang control is the fastest algorithm but also the least efficient one. It is not smooth enough to adapt itself to object shapes and can crush them. As explained in [15], the shooting function of the bang-bang controller is usually regularized with additional controllers. However, bang-bang control can be used to grab heavy objects. The higher the PAM pressure, the slower the PAMs contract, which is why their elasticity automatically opposes the shooting function.

BSC may be the most accurate algorithm, but is also the slowest one. As for PID control, BSC permits the fingers to adapt to the shape of objects with backward movements. Nevertheless, through the use of proportional and integrative controls, PID loops allow the fingers to move faster. The combination of PID control and SMC results in the accelerated rising time with SMC. As for conventional SMC, BSC depends on derivative and double derivative controls. This is the reason why the grasping time is much higher with the BSC, as it is not combined with proportional or integrative controls. Therefore, it takes 0.39 sec for the fingers to stabilise themselves with BSC, against 0.23 sec for SMC, 0.25 sec for PID control and

0.20 sec for bang-bang control. Indeed, as for SMC, the main advantage of BSC is its ability to regulate nonlinear actuators. This is the reason why these two algorithms receive feedback from pressure or position sensors, as in [16]. Nevertheless, in our case, the feedback is received from force sensors directly implemented on the mechanical structure instead of the actuators themselves, as in previous research [17][18].

Conclusion

This paper presents a feasibility analysis for combining conventional controllers with neural networks. While conventional methods such as PID control are widely used and have been found to be reliable, combining them with artificial intelligence approaches offers better accuracy rates. All the tests are carried out on a novel 3D printed multi-finger ambidextrous robot hand. Force sensors are used to trigger the algorithm. The grasping trajectory of each finger is combined with data with the adjacent fingers to improve accuracy. Tables 1 to 4 and Figs. 5 and 6 show the finger force against time and angle. Table 5 presents testing results. Neural Networks are found to be useful in control applications and could be used as a safeguard against conventional controller failure.

Acknowledgment

The authors would like to cordially thank Anthony Huynh, Luke Steele, Michal Simko, Luke Kavanagh and Alisdair Nimmo for their contributions in the project.

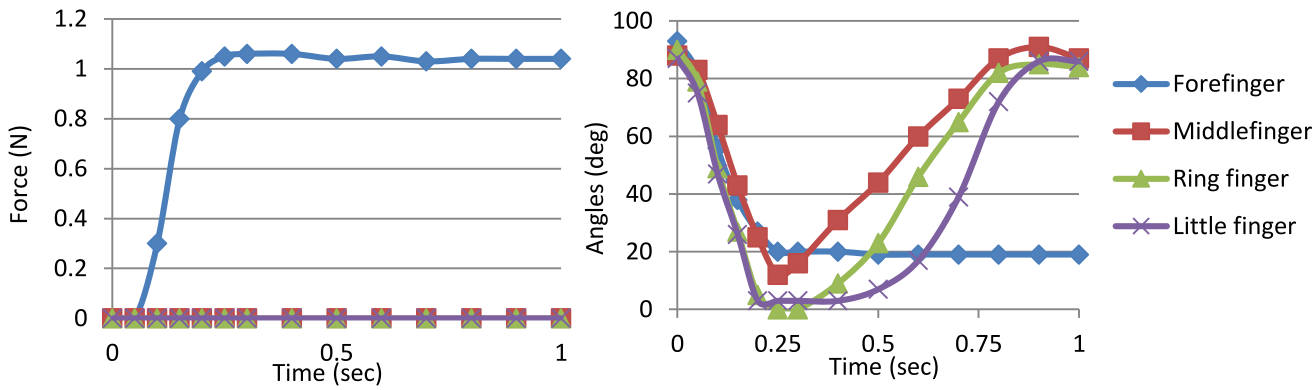

(a) (b)

Figure 6. Finger forces and angles against time when the hand grabs a ball.

Table 5. Performance comparison of conventional controllers when combined with NN.

Grasping algorithms	Algorithms to which it is combined	Averaged rising time (sec)	Averaged % of overshoot	Averaged	Averaged grasping time (sec)	Averaged settling time (sec)
SMC	PID, PPSC	0.20	N/A	0	0.23	0.23
PID	NN	0.16	5.3%	0	0.20	0.25
Bang-bang	Proportional, NN	0.10	40%	0	0.15	0.20
BSC [14]	NN	0.29	2.3%	0	0.37	0.39

References

[1] S. Jagannathan, A. Yesildirak, and F. W. Lewis, Neural Network Control Of Robot Manipulators And Non-Linear Systems, London: Taylor & Francis , 1999.

[2] G. Bekey, H. Tomovic, and W. Karplus, "Knowledge-Based Control of Grasping in Robot Hands Using Heuristics from Human Motor Skills," *IEEE Transactions on Robotics and Automation,* vol. 9, no. 6, pp. 709-721, 1993. doi: 10.1109/70.265915

[3] N. Xi, T. J. Tarn, and A. K. Bejczy, "Intelligent Planning and Control for Multi-robot Coordination: An Event-Based Approach," in proceeding of *IEEE International Conference on Robotics and Automation,* Atlanta, GA, May 02-06, 1993, pp. 439-445. doi: 10.1109/ROBOT.1993.291991

[4] L. Tian, J. Wang, and Z. Mao, "*Constrained Motion Control of Flexible Robot Manipulators Based on Recurrent Neural Networks," IEEE Transactions on*

Systems, Man, and Cybernetics—Part B (Cybernetics), vol. 34, no. 3, pp. 1541-1552, 2004. doi: 10.1109/TSMCB.2004.826400

[5] O. Adamiv, V. Koval, and I. Turchenko, "Predetermined movement of mobile robot using neural networks," in proceeding of *the Second IEEE International Workshop on Intelligent Data Acquisition and Advanced Computing Systems: Technology and Applications,* Lviv, Ukraine, Sept. 08-10, 2003. doi: 10.1109/IDAACS.2003.1249553

[6] H. Hashimoto, T. Kubota, M. Sato, and F. Harashima, "Visual Control of Robotic Manipulator Based on Neural Networks," *IEEE Transactions on Industrial Electronics,* vol. 39, no. 6, pp. 490-495 , 1992. doi: 10.1109/41.170967

[7] V. D. Smagt, P. Patrick, and J. A. Krose, "A Real-time Learning Neural Robot Controller," in proceeding of *the 1991 International Conference on Artificial Neural Networks, ICANN 91, FINLAND, 1991, pp. 351-356.* doi: 10.1.1.41.323

[8] G. Schram, F. Linden, B. Krose, and F. Groen, "Visual Tracking of Moving Objects Using a Neural Network Controller," *International Journal of Robotics and Autonomous Systems,* vol. 18, no. 3, pp. 293-299, 1996. doi: 10.1016/0921-8890(95)00084-4

[9] K. K. Ahn and H. P. H. Anh, "Design & Implementation an Adaptive Takagi-Sugeno Fuzzy Neural Networks Controller for the 2-Links Pneumatic Artificial Muscle (PAM) Manipulator using in Elbow Rehabilitation," in proceeding of *First International Conference on Communications and Electronics, 2006. ICCE '06*, Hanoi, Vietnam, Oct. 10-11, 2006, pp. 356-361. doi: 10.1109/CCE.2006.350793

[10] K. K. Ahn and N. H. T. Chau, "Intelligent Phase Plane Switching Control of a Pneumatic Muscle Robot Arm with Magneto-Rheological Brake," *Journal of Mechanical Science and Technology,* vol. 21, no. 8, pp. 1196-1206, 2007. doi: 10.1007/BF03179036

[11] H. Anh and N. Phuc, "Inverse Neural MIMO NARX Model Identification of Nonlinear System Optimized with PSO," in proceeding of *Fifth IEEE International Symposium on Electronic Design, Test and Application, 2010. DELTA '10,* Ho Chi Minh City, Vietnam, Jan. 13-15, 2010, pp. 144-149 . doi: 10.1109/DELTA.2010.61

[12] M. Mukhtar, E. Akyürek, T. Kalganova, and N. Lesne, "Implementation of PID, bang-bang and backstepping controllers on 3D printed ambidextrous robot hand," in proceeding of *Intelligent Systems and Applications*, Springer International Publishing Switzerland, 2016, pp. 173-194. doi: 10.1007/978-3-319-33386-1_9

[13] E. Akyürek, A. Huynh, and T. Kalganova, "Control of an Asymmetrical Design of a Pneumatically Actuated Ambidextrous Robot Hand," *International Journal of Electrical, Electronics, Communication, Energy Science and Engineering,* vol. 8, no. 5, pp. 782-787, 2014. dai: 10.1999/1307-6892/9998311

[14] M. Mukhtar, E. Akyurek, T. Kalganova, and N. Lesne, "Control of 3D printed ambidextrous robot hand actuated by pneumatic artificial muscles," in proceeding of *SAI Intelligent Systems Conference (IntelliSys), 2015,* London, UK, Nov. 10-11, 2015, pp. 290-300. doi: 10.1109/IntelliSys.2015.7361158

[15] C. Silva and E. Trélat, "Smooth Regularization of Bang-Bang Optimal Control Problems," *IEEE Transactions on Automatic Control,* vol. 55, no. 11, pp. 2488-2499, 2010. doi: 10.1109/TAC.2010.2047742

[16] H. Aschemann and D. Schindele, "Nonlinear Model-Based Control of a Parallel Robot Driven by Pneumatic Muscle Actuators," *New approaches in Automation and Robotics,* edited by H. Aschemann, I-Tech Education and Publishing, 2008. doi: 10.5772/5386

[17] E. Akyürek, T. Kalganova, M. Mukhtar, L. Steele, M. Simko, A. Nimmo, L. Kavanagh, L. Paramonov, A. Huynh, and Stelarc, "A novel design process of low cost 3D printed ambidextrous finger designed for an ambidextrous robotic hand," *WSEAS Transactions on Circuits and Systems*, vol. 14, art. 55, pp. 475-488, 2015.